

Spatially mapping random lasing cavities

R. C. Polson^{1,*} and Z. V. Vardeny¹

¹*Department of Physics and Astronomy, University of Utah, USA*

(Dated: April 2010)

Abstract

A mapping technique is developed to spatially resolve random laser emission spectra from disorder solid media with optical gain above the threshold excitation intensity for lasing; the technique is applied to π -conjugated polymer lms. By mapping the spatial extent of emission peaks in the random laser spectrum, bright areas that correspond to naturally-formed lasing microcavities are unraveled. The size of the obtained microcavities matches the size extracted from the Fourier transform analysis of the laser emission spectrum. Mapping at increased excitation intensities show multiple resonant microcavities that lase at increasing threshold intensities.

PACS numbers: 140.3580, 140.3945, 290.4210, 310.2790

*Electronic address: rpolson@physics.utah.edu

Lasers are typically thought of as a carefully constructed configuration of gain medium and resonance feedback. Typical lasers include everything from hand held pointers to room filling terawatt systems used to stimulate nuclear fission. However there exists a class of lasers where one can literally shake up the required components yet coherent laser emission emerges [1]. These diverse systems fall in the category of 'random lasers' (RL) and span from semiconductor power dye and scatterers [3], clusters of nanoparticles [4], dye infiltrated opals [5], stacks of dye and glass slides [6], dye and liquid crystals [7], nanoporous structures filled with optical gain [8] as well as π -conjugated polymer films [9]. One of the important open questions in the random lasing field is the mechanism by which the disorder gain medium produces *coherent emission*. Hints of how this occurs have recently been published [10, 11]. In this contribution we show an imaging technique that helps unravel the origin of this curious type of coherent laser emission.

As a disorder gain medium in our RL experiments we used a thin film of poly(phenyl vinylene) [PPV] derivative, namely poly(2,5-dihexyloxy-p-phenylenevinylene) (DHOPPV) that we synthesize in house [12]. The as synthesized dry polymer powder was mixed in toluene (~ 8 mg/mL), and subsequently the solution was heated at high temperature ($\sim 150^\circ\text{C}$) until the polymer was completely dissolved. The solution was then allowed to cool to room temperature, and then spun cast onto a glass substrate to form a neat polymer film. The optical excitation in our measurements was a laser beam from a picosecond (ps) Nd:YAG regenerative amplifier with ~ 120 ps pulse duration operating at ~ 800 Hz. We used the second harmonic at 532 nm to pump the sample film above the polymer optical gap. The film excitation was done in a dynamic vacuum ~ 300 mT in order to slow down the known film optical degradation due to photo-oxidation in air.

In order to resolve the *spatial extent* from which RL is emitted we used the novel method of space/spectrum cross-correlation (SSCC) of the laser emission [11], based on a spectrometer equipped with a microscope objective. The excitation beam was focused onto the polymer film using a spherical singlet lens. The emission (red) was collected with a 10x infinity-corrected microscope objective, and the laser excitation (green) was blocked with a long-pass filter. A third lens, which was mounted on a computer controlled translation stage, was used to couple the collected light to a spectrograph (see Fig. 1 (a)). The emission light was dispersed with the imaging spectrograph, and the light was recorded with a two dimensional (2D) CCD camera. The output of the CCD camera was slit-height, \mathbf{h} vs. wavelength, λ , where each

binned pixel covered ~ 10 microns in height with a wavelength resolution of 0.02 nm.

One of the characteristics of random lasing is that the spectrum changes when the a different area is excited [13]. In order to probe the emission from an excited area, we held fix the excitation spot, sample, and microscope objective; therefore translating the third lens adjusts which segment of the excited area is imaged by the spectrograph and CCD camera. By translating the third lens in the bf x-direction, different regions of the same excited film area can be therefore probed; at each X-value the CCD image records a 2D $[h, \lambda]$ array. Because of the 10x magnification, a lens translation, δX of 50 microns corresponds to 5 microns on the sample. We repeated the imaging process at many X values to form an emission image $I(h, \lambda, X)$. The SSCC method was recently used to show threshold dependence of lasing in a polymer lm [11], and a different method was also used where the entire spectrum was recorded and an optical image was obtained[10].

Figure 1 b shows RL emission spectrum from a polymer film pumped at excitation threshold, $I_{th} = 0.6\mu$ j/pulse. In this case all of the columns from the CCD image are summed over slight height , h, to give a spectrum of the integrated emission intensity. We note that the obtained RL emission peaks are very narrow; in fact they resemble true laser modes obtained in the laser emission spectra of polymer microrings and microdisks [12, 14]. The RL spectrum shown in Fig. 1(b) is not unique to π -conjugated polymer films; the emission spectra of other disordered gain media have also shown very narrow RL modes [4, 4, 15] .

We could assign the various narrow emission modes at I_{th} to Bessel functions, by applying the same analysis procedure as previously performed on laser spectra from photolithographic-prepared polymer microdisks [14] . The power Fourier transform (PFT) of the RL emission spectrum is calculated and shown in Fig. 1(c). The peaks in the PFT may provide a numeric value for the product nD of index of refraction and the diameter ,D, of a possible random microcavity responsible fro the RL spectrum. Using the relation $d = nD/2$ where d is the periodicity obtained in the PFT. From the PFT in Fig. 1 (c) the main Fourier component we get $nD = 106\mu m$; taking $n = 1.8$ [16] this exercise gives $D = 59\mu m$ for possible RL cavity size. With this value, predicted laser mode wavelength can be calculated corresponding to a zero of a Bessel function [12]. Most of the peaks in the RL spectrum can be thus assigned to families based on either rst zero of a Bessel function that is characterized by a single radial intensity maximum inside the cavity, or second zero having two radial intensity maxima. As seen in 1(b) the sharp modes agree very well to

series of successive Bessel functions; this is a strong indication for a random cavity with circular shape underlying the RL emission in the film.

Circular resonance cavities in a random medium are somewhat surprising. However, there are several theoretical works which argue that random cavities in fact should take a circular shape [17, 18]. The narrow peaks observed have been modeled as resulting from long scattering paths[19], or resulting from extended modes in a 2D system [20], or how multiple scattering increases a photon's time within a medium [21]. The polymer film has no inherent confinement in the plane and differs from gain filled photonic fiber [22] or long fiber lasers with scattering [22–24].

The integrated RL emission spectrum at two film locations, figure 2(a), shows the emission spectra summed over slit height for stage locations $X = 50\mu\text{m}$ and $X = 175\mu\text{m}$. The two RL spectra are very similar. The data set $I(\lambda, h, X)$ allows some processing to tease out further information about the location in the lm from which the emission originates. The main peak in Fig. 2 a is at $\lambda_0 = 633.5\text{ nm}$. It is possible to take the integrated intensity of the peak with $\Delta\lambda = 0.81\text{ nm}$ wide window, in order to calculate the emission peak intensity $I(\lambda_0 \pm \Delta\lambda, h, X)$. The resulting false-colored 2D image is shown in Fig. 2 (b). The λ_0 mode is most intense near $X = 50$ microns (namely row #10) in the center of the image; however it persists throughout most the excited film area, probably due to stimulated emission (SE) that is wave-guided inside the 2D-like polymer film.

The same area of film is scanned at a different excitation intensity $I > I_{th}$. Figure 3 (a) shows the emission spectra for the same two locations, $X = 50\mu\text{m}$ and $X = 175\mu\text{m}$, again the spectra are obtained by summing over the slit height for the two locations of the stage. The associated laser mode map at λ_0 but for $I = 2.8I_{th}$, $1.8\mu\text{J}/\text{pulse}$ is shown in 3 (b) . The emission spectra are again similar at these two position on the film, but not the same (notice minor peaks near $\lambda = 630\text{ nm}$). They are still narrow peaks, but there is a much stronger background due to amplified spontaneous emission (ASE) trapped in the film waveguide[9]. The mode map shows a different picture than that obtained at the lower intensity 2(b). In Fig. 3 (b) the emission is strong in an area to the left in a circular region; and there is a second region on the right that also has strong intensities. The size of the bright region on the left is roughly $50\mu\text{m}$ wide (ΔX) and $80\mu\text{m}$ (Δh) high. The bright spot agrees quite well with $D = 59\mu\text{m}$ for the cavity diameter extracted from the PFT analysis in figure 1 c. We showed above that the emission peaks can be described using circular Bessel

functions, and now in an independent determination we find that the seed emission area is also roughly circular. We thus conclude that the circular area is in fact a microresonator that is formed within the random polymer film. Earlier works utilized an average PFT over many locations to extract a mean cavity size [13, 15]. Integrated emission spectra over the entire lasing area were used, and then the excited area was translated many times on the film. Our present work demonstrates the existence of a single dominant resonator at $I \approx I_{th}$, in agreement with more direct pictures of the illuminated film area [11].

Using the RL mapping procedure at increasing excitation intensities we can now propose a framework to describe random lasing in π -conjugated thin films that incorporates many disparate facts. Starting with Fig. 2 at low excitation intensities only high Q-factor microcavities can overcome losses, and start lasing at relatively small I_{th} . Their SE is waveguided in the 2D-like polymer film into the surrounding excited gain medium; which, in turn may propagate back and thus further amplify the emission from the source microcavity. At this stage the emission spectrum from the polymer film appears to be nearly the same in the whole excited film area, because it originates from a localized seed microcavity region. At higher excitation intensities, as seen in Fig 3(b) separate microcavities cross lasing threshold and begin to emit their own emission [11]. However these microcavities are still seeded by the first dominant microcavity. The resulting emission is a combination of the intrinsic microcavity emission, the seeded emission, and an ASE background.

Acknowledgments

We thank L. Wojcik for the polymer synthesis. This work was supported in part by the DOE Grant No. DE-FG02-05ER03172 and the NSF DMR Grant No. 08-03325 at the University of Utah.

I. FIGURE CAPTIONS

Figure 1 (Color on line) (a) Schematic of the experimental set-up for imaging random laser. L1-L3 are lenses; S is the sample film; Sp is a spectrometer; and CCD is a charge-coupled device camera. (b) Integrated emission spectrum from $X = 50\mu m$. The red diamonds (green triangles) are calculated wavelengths based on an assumption of an underlying

circular microcavity having diameter $D = 59 \text{ m}$ (see text) (c) Power Fourier transform of the emission in (b)

Figure 2. (Color on line) (a) Random laser spectrum from positions $50 \mu\text{m}$ and $175 \mu\text{m}$ with excitation intensity, $I = I_{th} = 0.6 \mu\text{J} / \text{pulse}$. (b) Mapping intensity of the 633.5 nm mode as indicated by the grey band in (a).

Figure 3 (Color on line) Same as in Fig. 2 but for $I = 2.5I_{th}$.

-
- [1] D. S. Wiersma, Nat Phys **4**, 359 (2008).
 - [2] C. Gouedard, D. Husson, C. Sauteret, F. Auzel, and A. Migus, J. Opt. Soc. Am. B. **10**, 2358 (1993).
 - [3] N. Lawandry, B. R. M, A. Gomes, and E. Sauvain, Nature **368**, 436 (1994).
 - [4] H. Cao, Y. G. Zhao, S. T. Ho, E. W. Seelig, Q. H. Wang, and R. P. H. Chang, Phys. Rev. Lett. **82**, 2278 (1999).
 - [5] S. Frolov, Z. Vardeny, A. Zakhidov, and R. Baughman, Optics Communications **162**, 241 (1999).
 - [6] V. Milner and A. Z. Genack, Phys. Rev. Lett. **94**, 073901 (2005).
 - [7] G. Strangi, S. Ferjani, V. Barna, A. De Luca, C. Versace, N. Scaramuzza, and R. Bartolino, Optics express **14**, 7737 (2006).
 - [8] K. L. van der Molen, R. W. Tjerkstra, A. P. Mosk, and A. Lagendijk, Physical Review Letters **98**, 143901 (2007).
 - [9] S. V. Frolov, Z. V. Vardeny, K. Yoshino, A. Zakhidov, and R. H. Baughman, Phys. Rev. B **59**, R5284 (1999).
 - [10] J. Fallert, R. J. B. Dietz, J. Sartor, D. Schneider, and C. K. H. Kalt, Nature Photonics **3**, 279 (2009).
 - [11] A. Tulek, R. C. Polson, and Z. V. Vardeny, Nature Physics **6**, 303 (2010).
 - [12] R. C. Polson, G. Levina, and Z. V. Vardeny, Applied Physics Letters **76**, 3858 (2000).
 - [13] R. Polson, M. Raikh, and Z. Vardeny, Selected Topics in Quantum Electronics, IEEE Journal of **9**, 120 (2003).
 - [14] R. C. Polson, Z. V. Vardeny, and D. A. Chinn, Applied Physics Letters **81**, 1561 (2002).
 - [15] R. C. Polson and Z. V. Vardeny, Physical Review B (Condensed Matter and Materials Physics)

71, 045205 (2005).

- [16] A. Tulek and Z. V. Vardeny, *Applied Physics Letters* **91**, 121102 (2007).
- [17] V. M. Apalkov, M. E. Raikh, and B. Shapiro, *J. Opt. Soc. Am. B* **21**, 132 (2004).
- [18] V. M. Apalkov, M. E. Raikh, and B. Shapiro, *Phys. Rev. Lett.* **89**, 016802 (2002).
- [19] S. Mujumdar, M. Ricci, R. Torre, and D. S. Wiersma, *Phys. Rev. Lett.* **93**, 053903 (2004).
- [20] C. Vanneste, P. Sebbah, and H. Cao, *Phys. Rev. Lett.* **98**, 143902 (2007).
- [21] A. A. Chabanov, Z. Q. Zhang, and A. Z. Genack, *Phys. Rev. Lett.* **90**, 203903 (2003).
- [22] C. J. S. de Matos, L. de S. Menezes, A. M. Brito-Silva, M. A. Martinez Gámez, A. S. L. Gomes, and C. B. de Araújo, *Phys. Rev. Lett.* **99**, 153903 (2007).
- [23] J. Ania-Castañón, T. Ellingham, R. Ibbotson, X. Chen, L. Zhang, and S. Turitsyn, *Physical review letters* **96**, 23902 (2006).
- [24] S. Turitsyn, S. Babin, A. El-Taher, P. Harper, D. Churkin, S. Kablukov, J. Ania-Castañón, V. Karalekas, and E. Podivilov, *Nature Photonics* **4**, 231 (2010).

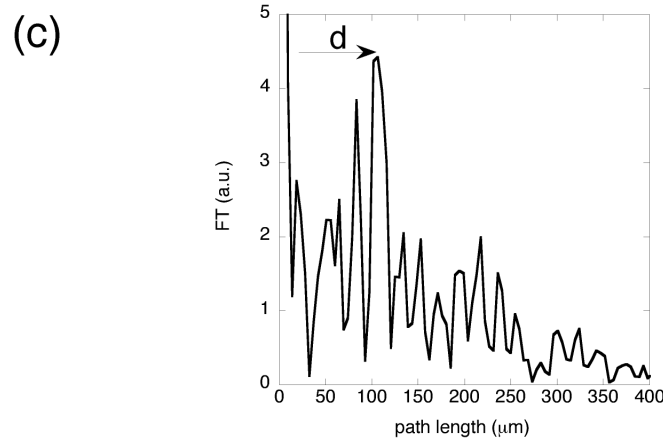
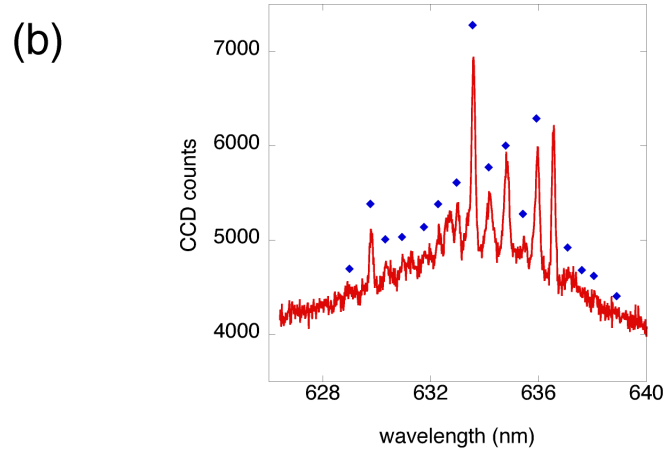
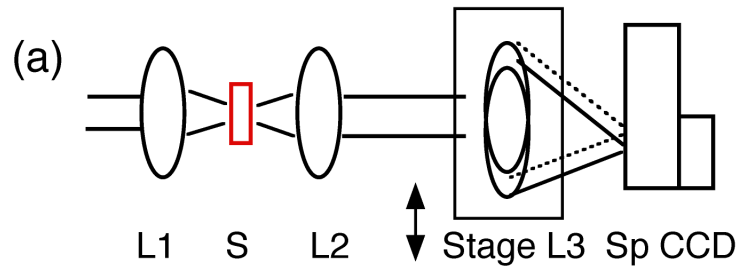


FIG. 1: (Color on line) (a) Schematic of the experimental set-up for imaging random laser. L1-L3 are lenses; S is the sample film; Sp is a spectrometer; and CCD is a charge-coupled device camera. (b) Integrated emission spectrum from $X = 50\mu\text{m}$. The red diamonds (green triangles) are calculated wavelengths based on an assumption of an underlying circular microcavity having diameter $D = 59\text{ m}$ (see text) (c) Power Fourier transform of the emission in (b).

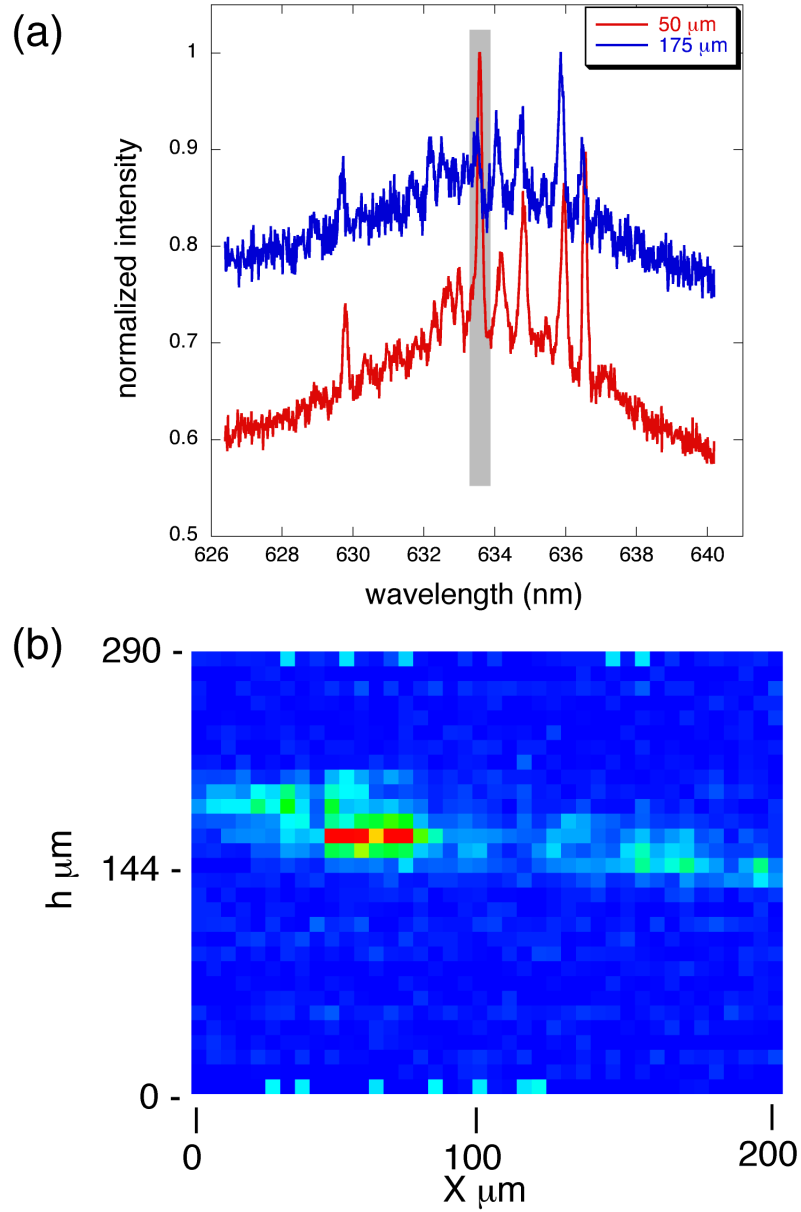


FIG. 2: (Color on line) (a) Random laser spectrum from positions $50 \mu m$ and $175 \mu m$ with excitation intensity, $I = I_{th} = 0.6 \mu J / \text{pulse}$. (b) Mapping intensity of the 633.5 nm mode as indicated by the grey band in (a).

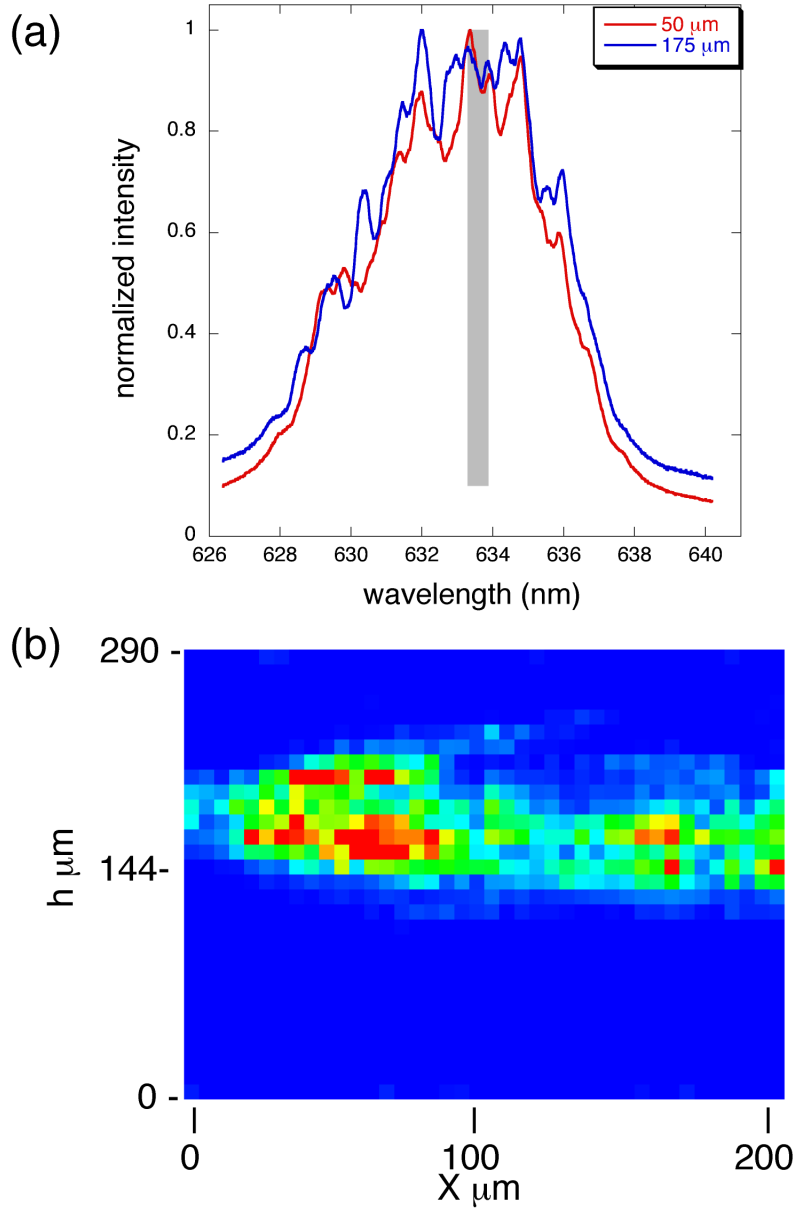


FIG. 3: (Color on line) Same as in Fig. 2 but for $I = 2.5I_{th}$.